Energy Advances

ROYAL SOCIETY OF CHEMISTRY

PERSPECTIVE

View Article Online
View Journal | View Issue

Cite this: *Energy Adv.*, 2025, 4, 1412

Advancing Fe–N–C catalysts: synthesis strategies and performance enhancements for fuel cell applications

Bochen Li[ab] and Rhodri Jervis *[ab]

Fe–N–C catalysts have emerged as the most promising class of non-precious metal electrocatalysts for the oxygen reduction reaction (ORR) in proton exchange membrane fuel cells (PEMFCs), offering favourable activity, structure tunability, and cost-effectiveness. However, challenges remain in achieving the performance and durability required for practical applications. This review systematically summarizes recent progress in Fe–N–C catalyst development, with a focus on synthetic strategies aimed at increasing the active site density, optimizing Fe–N_x coordination environments and potential engineering solutions to the membrane electrode assembly (MEA) based on Fe–N–C, particular attention is given to the pyrolysis atmosphere control, post-synthesis treatment, and optimizing the microstructure and catalytic performance. Furthermore, this review explores emerging approaches to integrate Fe–N–C catalysts into membrane electrode assemblies (MEAs), including ionomer–catalyst interaction tuning and electrode architecture optimization, with the goal of bridging the gap from laboratory activity to real-world fuel cell operation.

Received 4th September 2025,
Accepted 4th November 2025

DOI: 10.1039/d5ya00256g

rsc.li/energy-advances

1. Introduction

The ever-growing energy demand driven by the increasing population, technological and industrial development has resulted in many environmental and economic challenges, including air pollution, global warming, and local conflicts caused by fluctuation in oil price and resource scarcity. Currently, fossil fuel-based energy reserves can meet human demands, but the excessive use of remaining fossil fuels is one of the main contributors to global warming. The combustion of fossil fuels releases large amounts of greenhouse gases, exacerbating global temperature rise and climate change. Therefore, fossil fuels should be used more as precursor chemicals rather than being directly burned, in order to reduce their negative impact on the environment.[1] Despite renewable energy sources, especially wind and, solar, experiencing significant proliferation, their unpredictability prevents us from relying on them fully. Alongside renewable generation, green energy transfer and storage technologies are vital to develop in tandem. Hydrogen is a clean energy carrier that produces only water as product when used as a fuel. Fuel cells, characterized by their high energy conversion efficiency and energy density, are particularly important as zero-carbon emission devices, making them highly promising for supporting the transition of the energy system towards carbon neutrality by 2050.[2]

Proton exchange membrane fuel cells (PEMFCs) are the most successfully commercialized and practically applied type of fuel cells to date, with the Toyota Mirai being one of the most representative automotive examples.[3] The commercial competitiveness of fuel cells largely depends on their cost, with the Pt based catalyst being the most significant contributor-accounting for approximately 41% of the total cost of a fuel cell stack,[4] which, coupled with significant infrastructure requirements, has made them uncompetitive with Li ion battery electric vehicles for personal automotive in recent years. Since Jasinski's discovery that Metal–N_x sites in metal phthalocyanines in 1960s can catalyse the oxygen reduction reaction (ORR) in alkaline electrolytes, extensive efforts have been devoted to developing non-precious catalysts in order to reduce the cost of fuel cells.[5–7] Among various transition metals, Fe–N_x sites have demonstrated superior catalytic activity. Fe–N–C materials, constructed by embedding atomically dispersed Fe centers into a nitrogen-doped carbon matrix, have emerged as promising non-precious metal catalysts for the ORR at fuel cell cathodes. ZIF-8 is commonly used as a precursor due to its high nitrogen content, controllable structure, and the easy removal of Zn during pyrolysis. The atomic dispersion of Fe atoms not only guarantees a high density of accessible catalytic sites but also tailors the local coordination environment, which strengthens the interaction between Fe centres and oxygen intermediates,

[a] *Electrochemical Innovation Lab, Department of Chemical Engineering, University College London, London WC1E 7JE, UK*
[b] *Advanced Propulsion Lab, Department of Chemical Engineering, University College London, London, WC1E 6BT, UK*

thereby maximizing metal atom utilization and efficiency.[8] Furthermore, precise modulation of the local coordination environment enables the rational design of active sites, selectively steering reaction pathways and ultimately enhancing catalytic performance.[9] Nonetheless, under the acidic conditions required by PEMFCs, Fe–N–C catalysts still fall short of the performance of Pt-based catalysts, especially in terms of activity and durability. Although Fe–N–C catalysts have shown good activity in alkaline media, the practical application of alkaline fuel cells is limited by the lack of suitable membranes. As a result, efforts toward advancing Fe–N–C catalysts are predominantly focused on acidic conditions, which align with the operational environment of commercially relevant PEMFC technologies. Therefore, this perspective aims to explore recent strategies and fundamental insights for improving the performance of Fe–N–C catalysts in acidic environments, with the ultimate goal of enabling their practical application in next-generation PEMFC systems.

2. Current strategies for improving Fe–N–C catalysts for the oxygen reduction reaction

Typically, the primary active sites of Fe–N–C catalysts for the oxygen reduction reaction (ORR) are FeN_4C_{12} and FeN_4C_{10} moieties, which correspond to pyrolic- and pyridinic-N coordinated configurations, respectively, as illustrated in Fig. 1. The former (FeN_4C_{12}) exhibits superior catalytic activity but suffers from undesirable degradation due to severe irreversible Fe demetallation, leading to the formation of iron oxides. In contrast, the latter (FeN_4C_{10}) shows slightly lower activity but offers enhanced structural stability,[10–12] and it also suppresses H_2O_2 formation by tunning *OOH binding to favor O–O cleavage ($4e^-$ pathway) over *OOH desorption ($2e^-$ to H_2O_2).[13] This section discusses the activity–stability trade-off between these two site types and explores strategies to enhance both performance and durability.

Under the acidic and oxidising environment of PEMFCs, Fe–N–C catalysts deactivate through 3 main pathways, which are most consequential at the atomistic level.

(i) Demetallation of Fe–N sites: under acidic media and cathodic potentials relevant to the ORR, protonation of the coordinating nitrogens weakens the Fe–N bonds.[14] Once two adjacent N atoms are protonated, the Fe centre may migrate away from the original N_4 cavity, usually while being ligated by oxygen-containing adsorbates, and ultimately dissolve as Fe^{2+}/Fe^{3+}, or reprecipitate as iron oxides.[15] Operando and post-mortem analyses commonly detect the irreversible loss of atomically dispersed Fe together with the appearance of FeO_x phases, which directly reduces turnover capacity, and drives the reaction toward 2-electron pathway.[16]

(ii) Carbon corrosion: the active Fe–N site in Fe–N–C catalysts is embedded within a carbon matrix, and the structural integrity of this carbon support is critical for long-term catalyst stability. Electrochemical carbon corrosion can occur at above 0.207 V_{RHE}, and is significantly accelerated during start-up/shut-down cycles, which accelerate oxidative carbon degradation.[17–19] Simultaneously, hydrogen peroxide and reactive oxygen species generated during ORR chemically attack defect-rich carbon regions, leading to C–C bond cleavage, loss of structural support, and ultimately Fe site destabilization and demetallation. Beyond ORR activity, carbon corrosion could result in reduced electronic conductivity and structural collapse of the cathode layer.[14] The degradation of the carbon network disrupts electron transport and gas diffusion, further lowing the fuel cell performance.

(iii) Chemical attack by hydrogen peroxide intermediates and radicals: Fe–N–C catalysts tend to generate a higher fraction of hydrogen peroxide during acidic ORR compared to Pt-based catalysts, due to partial oxygen reduction *via* the 2-electron pathway. H_2O_2 is oxidative and can directly attack Fe–N sites, alter their coordination environment and promote

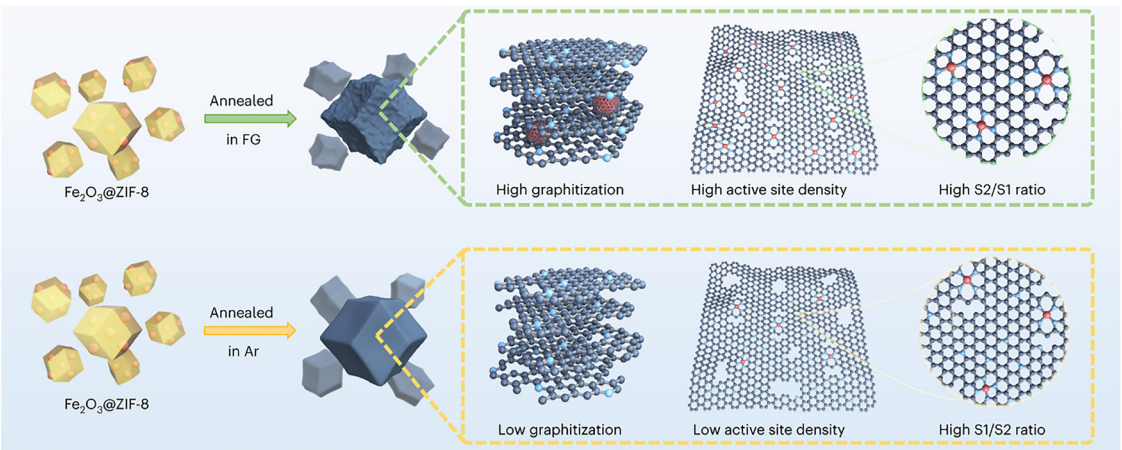

Fig. 1 Schematic of the construction of S1-pyrrolic and S2-pyridinic nitrogen sites through controlled pyrolysis atmosphere. Reproduced with permission.[22] Copyright © 2023 Springer Nature Limited.

Fe leaching. More critically, in the presence of Fe^{2+}/Fe^{3+}, H_2O_2 undergoes Fenton-like reactions to form highly reactive hydroxyl and peroxyl radicals. These species could oxidize surrounding carbon and break Fe–N bonds.[20] Kinetic analyses by Yin and Zelenay *et al.* suggest that the rapid initial performance loss of Fe–N–C catalysts follows a self-catalysed decay mechanism, driven by this radical feedback loop: peroxide formation leads to Fe dissolution, which then accelerates further radical generation and structural damage.[21] At the molecular scale, this autocatalytic process represents a major pathway of active site degradation and carbon corrosion and is considered a central challenge limiting Fe–N–C durability in PEMFC.

2.1. Hydrogen treatment

Hydrogen treatment is one of the most widely adopted strategies which involves introducing a small amount of hydrogen gas (typically 5–10%) mixed with an inert gas during the pyrolysis of the Fe–N–C precursor, as comprehensively studied by Zeng *et al.*, who pyrolyzed a Zeolitic imidazolate framework-8 (ZIF-8)/Fe_2O_3 composite under different H_2/Ar concentrations[22] and obtained 720 mW cm^{-2} in a PEMFC under H_2–air conditions (150 kPa backpressure, 4 mg cm^{-2} loading, Gore membrane). ZIF-8, one of the most classical MOF precursors for Fe–N–C synthesis, is particularly suitable due to its high nitrogen and carbon content, well-defined porous structure, and thermal stability. Moreover, the zinc species in ZIF-8 possess a relatively low boiling point (907 °C), which facilitates partial evaporation during pyrolysis, contributing to the formation of porous structures and improved mass transport properties.[23,24] This treatment effectively removes most of the unstable pyrrolic-type sites and concurrently shortens the Fe–N bonds at both pyrolic and pyridinic sites by hydrogenating the carbon atoms adjacent to the active centres.[22] Hydrogen also helps eliminate poorly graphitised carbon and residual hetero elements. It increases the catalyst's graphitization, which suppresses carbon corrosion by raising the oxidation onset potential, improving electronic conductivity, and reducing defect/edge sites, thereby limiting radical ($^{\bullet}OH/^{\bullet}OOH/H_2O_2$) attack. On the other hand, although the pyrolysis temperature exceeds zinc's boiling point, hydrogen drives even more zinc out, creating additional micro and mesopores and enlarging the accessible surface area.[25,26] The resulting increase in pore volume is crucial for relieving mass-transport limitations in Fe–N–C cathodes used in fuel cells.

2.2. Ammonia/ammonium compound treatment

Ammonia (NH_3) treatment is also an effective strategy to enhance the activity of Fe–N–C catalysts. Ammonia serves not only as a reductive gas but also as an additional nitrogen source. During pyrolysis, NH_3 typically decomposes into N_2 and H_2 between 500 °C and 900 °C and further dissociates into highly reactive nitrogen and hydrogen atoms at temperatures above 900 °C.[27,28] These active atoms could react with poorly graphitised carbon to form HCN and CH_4, forming significant amount of micro-mesopores, which is the key for hosting the Fe–N_4 active.[29] Kramm *et al.* were the first to provide valuable guidance on the role of ammonia treatment in Fe–N–C electrocatalysts, using chloroirontetrametoxyphenylporphyrin (Fe(TMPP)Cl) as precursor and demonstrated how secondary ammonia pyrolysis influences FeN_4 site turnover frequency and porosity.[30] Under this atmosphere, the Fe–N_4 bonds can be strengthened, and the active sites can be redispersed. Moreover, any remaining Fe-based nanoparticles or clusters can react with nitrogen species to form new Fe–N coordination sites, thereby increasing the density of active centres.[31] Ammonia treatment functions much like hydrogen treatment, but with the added benefit of supplying extra nitrogen, thereby compensating for nitrogen loss during high-temperature pyrolysis and enhances both the catalytic activity and long-term stability (Fig. 2).

In addition, various analogous strategies have been developed by introducing specific additives that thermally decompose at high temperatures to release ammonia and other gases/compounds, which facilitate the formation of active sites and porous structures within the carbon matrix. For instance, melamine, with its high nitrogen content (67 wt% N), acts both as a nitrogen precursor and a soft template. It coordinates Fe ions to anchor atomically dispersed Fe–N_x centers and, upon

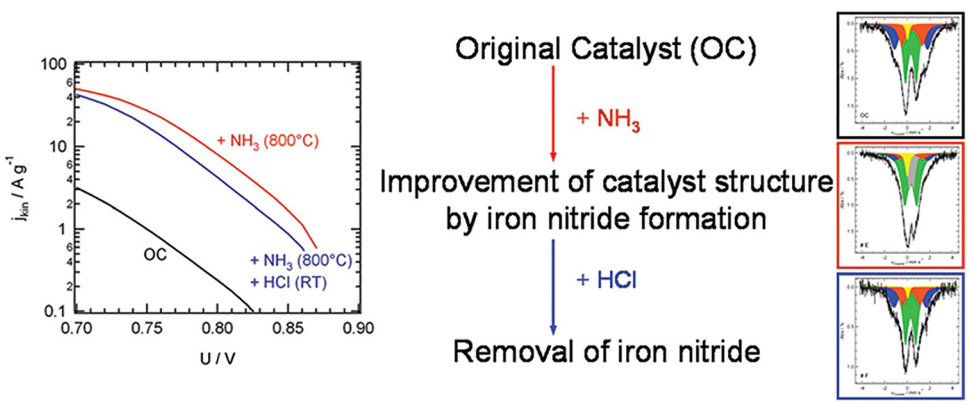

Fig. 2 Fe–N–C structural, Composition and ORR activity evolution of Fe–N–C catalyst upon NH_3 treatment. Reproduced with permission.[30] Reproduced with permission. Copyright © 2011 American Chemical Society.

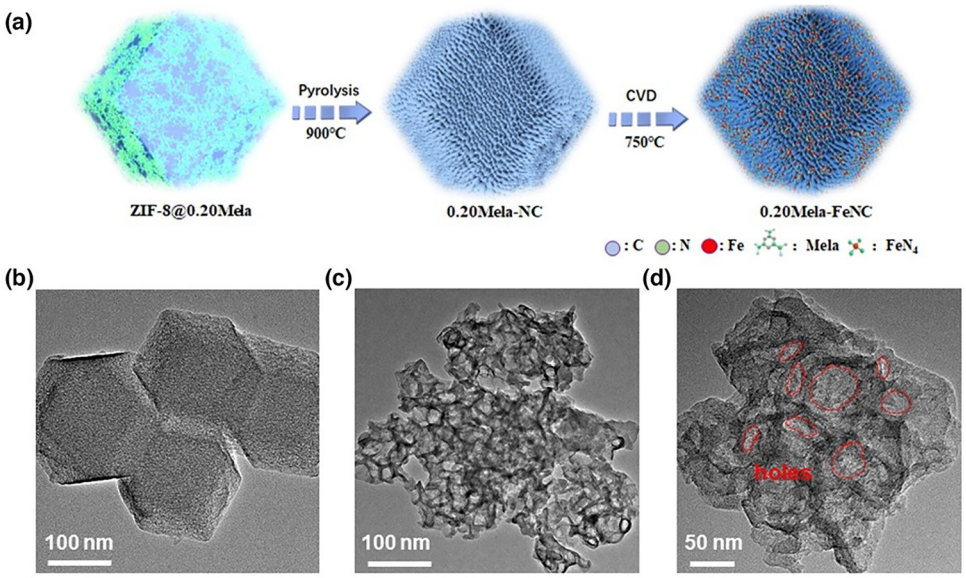

Fig. 3 (a) Schematic synthetic process of Fe–N–C with treatment of Melamine. TEM image of (b) Fe–N–C without Melamine treatment, (c and d) Fe–N–C with Melamine treatment.[33,34] Copyright © 2023 John Wiley&Sons, Inc or related companies.

heating, its condensation and decomposition release ammonia and HCN gases that etch micro-/mesopores and help remove poorly graphitized carbon.[32] Recently, Li *et al.* developed a melamine-assisted chemical vapor deposition method that achieves improved site density, utilization, and mass transport, demonstrating that melamine can effectively promote the formation of active sites and optimize the pore structure, achieving peak power density of 540 mW cm^{-2} in PEMFC under H_2–air conditions (200 kPa backpressure, Gore select membrane, 3.5 mg cm^{-2}).[33,34] This could be attributed to Melamine treatment providing effective site utilization and construction of the hierarchical pore structure (Fig. 3).

Beyond melamine, many other compounds have been investigated using different treatment methods, such as physical mixing followed by pyrolysis or chemical vapor deposition, including: 1,10-phenanthroline,[35] ammonium chloride,[36] ammonium iodine,[37] ammonium bromide(where Iodine and bromide can dope the catalyst surface),[38] cyanamide,[15] urea,[39] dicyandiamide[40] and others. Diverse additives offer multiple strategies to tailor the active site density, nitrogen incorporation, and pore architecture of Fe–N–C catalyst. These approaches primarily aim to increase the proportion of pyridinic nitrogen, modify Fe–N bond strength, either by shortening the bond length, increase the graphitization and/or introducing heteroatoms such as F or Br to alter the coordination environment, recduce the hydron peroxide production and increase the carbon corrosion, and ultimately provide a versatile toolbox for optimizing catalytic performance.

While significant progress has been achieved in improving the catalytic activity, site density, mass transport, and structural stability of Fe–N–C catalysts through strategies such as hydrogen and ammonia treatments, nitrogen-rich additives, and advanced synthesis techniques, several key challenges remain. Despite reported improvements in durability, most studies focus on short- to medium-term stability under laboratory conditions, whereas the long-term operational stability under realistic fuel cell environments (such as acidic media, high potentials, and dynamic cycling) requires further investigation. Moreover, the mechanistic understanding of how specific treatments (*e.g.*, ammonia-induced active site redistribution, bromide doping, or additive-driven pore formation) enhance catalyst stability at the atomic scale remains incomplete. In the future development of Fe–N–C catalysts, a deeper understanding of their atomic-scale degradation mechanisms will be essential to bridge the gap between laboratory activity and practical fuel cell durability. Current studies indicate that performance decay arises from interplay of Fe–N_4 demetallation, carbon matrix oxidation, and peroxide-induced radical attack, which occur simultaneously and often reinforce one another under operating conditions. To elucidate these coupled processes, future research should integrate advanced *in situ*/operando characterization techniques such as X-ray adsorption spectroscopy (XAS) and Mössbauer spectroscopy for Fe–N site dementalization, and Raman spectroscopy for carbon corrosion, with theoretical modelling approaches such as DFT and molecular dynamics simulation to capture the dynamic evolution of active sites under realistic PEMFCs operation. Moreover, establishing quantitative links between synthesis strategies (*e.g.*, pyrolysis atmosphere control, coordination tuning and support engineering) and specific degradation pathways will enable a mechanism-driven design framework beyond empirical optimization.[41] From a broader perspective, achieving long-term stability requires multi-scale integration - connecting atomic-level understanding with Membrane-electrode-assembly level electrode design. The convergence of mechanistic insight, rational synthesis and engineering control will ultimately lead to Fe–N–C catalysts that combine high

activity, durability and scalability, advancing the field toward viable PGM-free fuel cell commercialization.

3. Active site density increase

While considerable efforts have been made to improve the intrinsic activity and stability of Fe–N–C catalysts, these strategies alone are insufficient to meet the practical demands of high-performance fuel cells. Even when the active sites are highly optimized, the overall cathode performance often falls short, primarily because the low density of active sites requires the construction of thicker catalyst layers to achieve sufficient total site numbers. However, such thick layers hinder gas transport and increase the risk of electrode flooding, ultimately limiting the performance, particularly at the high current densities desired during operation.[42] Therefore, beyond the optimization of active site properties, the enhancement of overall catalyst loading, coupled with the preservation of high site accessibility and efficient mass transport, has emerged as a pivotal focus for advancing Fe–N–C catalysts from laboratory-scale studies toward practical applications. Most reported Fe–N–C catalysts achieve only <1.5 wt% Fe content, as single-atom metals possess intrinsically high surface energy, and excessive Fe precursors tend to aggregate into inactive nanoparticles or undesirable phases such as metallic Fe clusters, iron carbides, and iron nitrides during high-temperature pyrolysis.[43–47] Although various atmospheric conditions or additives (such as melamine, ammonium chloride) during the annealing process to improve Fe–N–C site formation can slightly increase the site density, it is still insufficient for practical applications. This chapter provides a comprehensive overview of recent advances in strategies designed to effectively increase Fe–N–C catalyst loading, with an emphasis on addressing the associated challenges and opportunities for future development.

3.1. Chemical vapor deposition strategy

Chemical vapor deposition (CVD) is a versatile gas-phase synthetic technique widely employed to deposit thin films or introduce atomically dispersed active sites onto solid substrates.[48] In the case of Fe–N–C catalysts, CVD enables Fe-containing vapours (such as $FeCl_3$) to diffuse and react with nitrogen-doped carbon substrates under elevated temperatures, anchoring Fe atoms as isolated Fe–N_4 sites.[49] Compared to conventional impregnation or solid-state mixing methods, CVD effectively minimizes Fe aggregation, enhances the dispersion of active sites, and allows for higher Fe loadings with maximized site utilization. For example, Li *et al.* reported the fabrication of dense Fe–N_4 site-rich Fe–N–C catalysts by vaporizing anhydrous $FeCl_3$ (boiling point 316 °C) in an upstream boat and depositing it onto Zn–N–C in a boat positioned downstream, achieving Fe content of 2 wt% and an impressive power density of 370 mW cm^{-2} in H_2–air PEMFC (150 kPa backpressure, Nafion 212 membrane, 6 mg cm^{-2} loading).[50] The choice of Fe precursor in CVD critically governs the vapor-phase transport, reaction kinetics, and ultimately the density

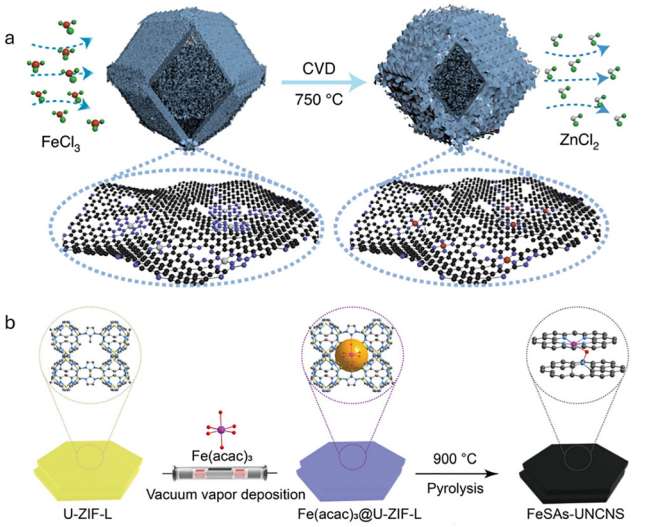

Fig. 4 Schematic CVD synthetic process of Fe–N–C of with (a) $FeCl_3$, Reproduce with permission.[50] Copyright © 2021 Springer Nature Limited. (b) $Fe(acac)_3$, Reproduce with permission.[51] Copyright © 2024 John Wiley & Sons, Inc or related companies.

and uniformity of Fe–N_4 active sites, highlighting the importance of precursor selection and process optimization. Different Fe sources can significantly affect the vapor-phase transport behaviour, reaction pathways, and potential side reactions during high-temperature processing. Yang *et al.* synthesized ultrathin Fe–N–C nanosheets from ZIF-L, which has the same structure as ZIF-8 but with a 2D morphology, using vacuum vapor deposition with iron acetylacetonate (*i.e.*, $Fe(acac)_3$, boiling point 187.6 °C) as the Fe source, with Fe loading of 4.22 wt%.[51] These two examples demonstrate that while the CVD method can effectively enhance the Fe loading in Fe–N–C catalysts, the selection of Fe precursors, including factors such as molecular size, boiling point, and volatility, plays a pivotal role in determining deposition efficiency and the distribution of active Fe–N_4 sites.[52] Further systematic investigations into precursor properties and their relationship with CVD processing conditions could provide valuable guidance for optimizing Fe utilization and improving overall catalyst performance (Fig. 4).

3.2. Impregnation strategy

While CVD offers precise control over Fe deposition by diffusing gaseous iron precursor into carbon support, the impregnation method represents another commonly used and more scalable strategy to increase Fe loading, relying on solution-based processes and post-synthesis activation. Typically, through immersing nitrogen-doped carbon substrates in Fe precursor solutions, the Fe^{3+} ion is not only adsorbed within the micro- and mesopores of the nitrogen-doped carbon substrate, but also effectively anchored by nitrogen atoms, which provide coordination sites that prevent aggregation during subsequent pyrolysis.[53] Additionally, oxygen vacancies present in the carbon framework could also promote the adsorption and stabilization of Fe species, enhance the overall dispersion and durability of the active sites.[54] For example, MOF-derived

N–C contains abundant nitrogen embedded in the carbon framework along with a high density of micropores, while reduced graphene oxide is rich in oxygen vacancies.[55,56] Here, particular attention is given to ZIF-8 derived Fe–N–C catalysts, due to their unique porous structure and high nitrogen content, and we review representative studies that have explored strategies to enhance Fe loading. Mehmood *et al.* modified the traditional impregnation method to increase the Fe loading to 7 wt% using commercial ZIF-8 as the precursor, achieving a peak power density of 429 mW cm^{-2} in a PEMFC under H_2–air conditions (150 kpa backpressure, Nafion 211 membrane, 100 kPa backpressure, 3.9 mg cm^{-2} loading).[40] The key strategy involved removing most of the Zn from the N–C framework by acid reflux to create enriched metal–vacancy–N_x sites, followed by a secondary reflux in an iron chloride methanol solution to fill these vacancies with Fe^{3+} ions, and finally pyrolyzing the catalyst to activate the catalytic sites. Expanding on this concept, Lan *et al.* reported a new record Fe–N–C catalyst with an Fe loading of 11.8 wt% with active site utilization of 79.8% was achieved using a similar strategy combined with a segmentally annealed process. The Fe-ion-adsorbed N–C was first annealed at 300 °C for 5 hours, followed by a second annealing stage at 700 °C for 4 hours.[57] The initial low-temperature treatment enhanced the interaction between the metal precursor and the carbon support, thereby effectively suppressing the aggregation of Fe atoms during the subsequent high-temperature activation.[58] Aberration-corrected HAADF-STEM imaging revealed only isolated bright spots attributable to single Fe atoms, with no observation of Fe nanoparticles or clusters. This observation was further confirmed by Fe k-edge XANES/EXAFS analysis, which showed Fe coordination environments consistent with Fe–N bonding and no detectable Fe-Fe coordination peak, verifying that all Fe species remained atomically dispersed. This represents a significant breakthrough, achieving a record-high loading while maintain excellent atomic dispersion and high active-site utilization. Although the study did not evaluate the catalyst in PEMFCs, the Zn–Air battery configuration clearly demonstrated the catalyst's superior activity and durability, confirming that the high Fe loading effectively translated into enhanced device-level electrochemical performance (Fig. 5)

3.3. Comparative critical analysis of CVD and impregnation-pyrolysis routes for Fe–N–C catalysts

The chemical vapor deposition (CVD) route is widely recognized as one of the most precise approaches for constructing Fe–N–C catalysts. The main advantage lies in its ability to deposit gaseous Fe precursors uniformly onto N-doped carbon support under controlled atmospheres, resulting in high-density and fully exposed Fe–N active sites. Compared with traditional wet-chemical methods, CVD provides better control over metal-nitrogen coordination and minimizes ion-diffusion-induced aggregation, thus achieving higher atomic utilization. In addition, CVD generally eliminates the need for post-synthesis acid leaching, which can reduce liquid waste generation. However, the main challenge in scaling up CVD lies in maintain process uniformity and engineering feasibility. When scaling from gram to kilogram batches, temperature and precursor partial-pressure gradients

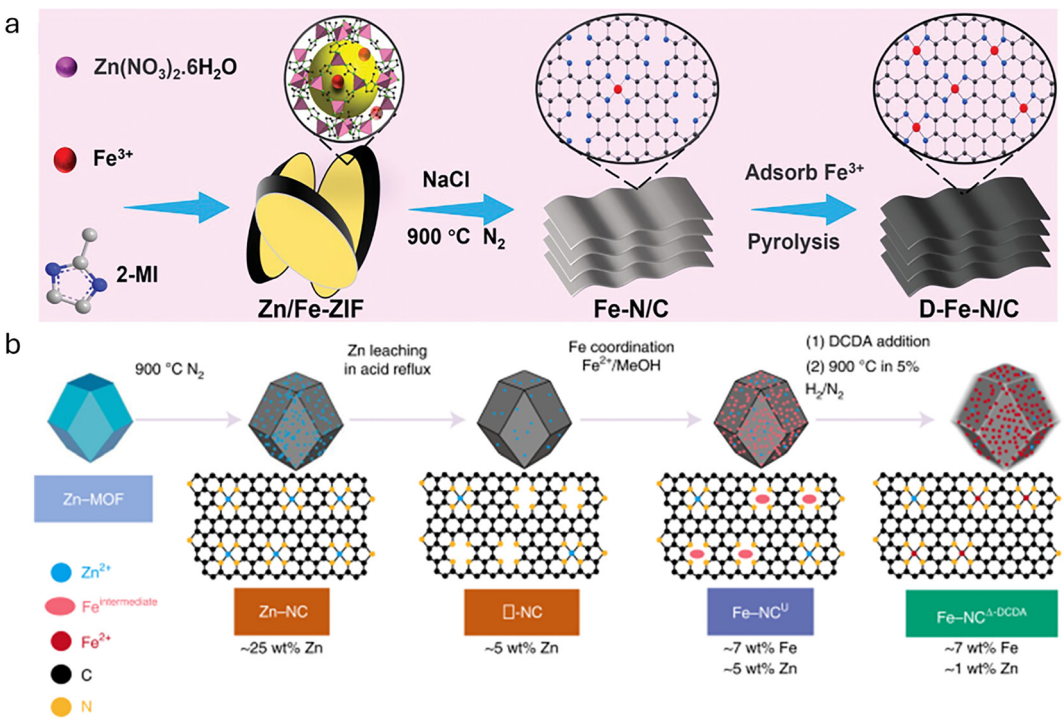

Fig. 5 Schematic impregnation synthetic process (a) one step anneal process, Reproduced with permission.[40] Copyright © 2021 Springer Nature Limited. (b) segmentally annealed process. Reproduce with permission.[57] Copyright © 2025 John Wiley & Sons, Inc or related companies.

inside the reactor cause non-uniform Fe- deposition, local aggregation, and reproducibility issues. The use or formation of corrosive gases such as $FeCl_3$ and NH_3 can corrode reactor material and lead to precursor/carbon deposits on the reactor wall, Therefore, the process demands corrosion-resistant reactors, precise flow control, regular cleaning and multi-stage exhaust treatment, leading to higher capital and operating cost and increased safety risks.[48] Although recent advances, including fluidized-bed CVD, rotary CVD and template assisted CVD, have been developed to improve gas distribution and site uniformity, no reliable kilogram-scale engineering validation has yet been achieved. Further progress should focus on the development of low-temperature, continuous CVD system to achieve a balanced integration between catalytic performance and engineering feasibility.

Compared with CVD, the impregnation method is currently the most practical and industrially adaptable route for synthesizing Fe–N–C catalysts. It stands out for its low-cost precursors, mature processing and compatibility with standard furnaces, allowing hundred-gram to kilogram-scale production with good batch to batch reproducibility. However, during scale-up, uneven heat and mass transfer in thick material layers can lead to Fe-migration and aggregation, forming inactive Fe or Fe_3C phases that reduce the proportion of Fe–N_4 sites.[59] In addition, acid leaching, while effective at removing in active species, can also dissolve part of the Fe–N_4 sites and generate acidic waste containing iron, creating environmental concerns.[60] Strategies mentioned in Section 2 could effectively improve Fe dispersion and reduce acid dependency. Overall, the impregnation method offers excellent scalability and economic efficiency, and future research should aim to integrate CVD-like structural precision to achieve a balance between catalytic performance and manufacturability (Table 1).

4. Catalyst layer engineering

MOF-derived carbon supports or catalysts typically struggle to achieve high performance in working fuel cells, even when combined with Pt-based nanoparticles on their surfaces. Encouraging performance metrics in ultra-low loading rotating disc electrochemical experiments often fail to translate into high current density/low-overpotential performance in a working fuel cell electrode. What limits the performance of MOF-derived materials in fuel cells is largely due to the pore structure of the carbon particles, which predominantly consist of micropores (<2 nm).[62] While the abundance of micropores contributes to a high surface area and increased exposure of active sites, it also creates significant mass transport challenges due to a shortage of meso- and macro- pores limited the reactant diffusion to the channel.[63] With only limited mesopores and macropores, micropores alone are insufficient to effectively facilitate the transport of gaseous reactants and the removal of accumulated water in the catalyst layer, potentially limiting overall catalytic efficiency.

4.1. Template strategies

A high-efficiency catalyst layer must give a hierarchical pore structure that provides not only a high surface area but also a balanced combination of micropores, mesopores, and macropores, which is important for the mass transport in PEMFCs. The hard-template method is a synthesis strategy that uses rigid, pre-formed solid materials (such as SiO_2, Al_2O_3, or $CaCO_3$) to shape the structure of target materials.[64] After deposition or formation of the desired material around the template, the template is removed, typically by chemical etching or calcination, leaving behind a porous or hollow architecture. Since Kui *et al.* introduced the polystyrene (PS) hard-templating strategy to fabricate ordered macro–microporous MOF single crystals, considerable effort has been devoted to incorporating such hierarchical structures into various applications.[65,66] Recently, several studies have focused on utilizing the hard-template method to construct porous structures in ZIF-8-derived carbon materials. For example, Zhai *et al.* synthesized a Fe–N–C single-atom catalyst supported on a hierarchically porous carbon framework using a PS sphere template. The resulting material featured a 3D-ordered macroporous structure with pore sizes around 160 nm, which significantly enhanced oxygen reduction reaction (ORR) performance by improving kinetic mass transport efficiency.[67] This underscores the importance of hierarchical pore structures in optimizing catalyst performance, highlighting their potential for application in fuel cells, where effective mass transfer and active site utilization are key to achieving high performance,[68] however, the hard-template strategies typically involved complex, costly syntheses, consequently, research has shifted toward soft-template approaches to simplify the process and reduce the costs (Fig. 6).

Compared with hard-template methods that use solid scaffolds and require additional removal steps, soft-template strategies

Table 1 Representative PEMFCs performance of Fe–N–C catalysts

Electrocatalyst	Catalyst layer loading (mg cm^{-2})	Membrane	Backpressure (kPa)	Peak power density (mW cm^{-2})	Ref.
Fe–N–C–FG	4	Gore	150	720	Nature Catalysis (2023)[22]
0.20 Mela-FeNC	3.5	Gore-Select	200	540	Energy & Environmental Materials (2023)[33]
Fe–N–C–CVM	3	Nafion 212	100	450	Nature Communication (2024)[15]
Fe–N–C–BrCl	3.5	Gore-Select	250	880	Nature Communication (2024)[38]
Fe–N–C-CVD-750	6	Nafion 211	150	370	Nature Material (2021)[50]
Fe–N–C–ΔDCDA	3.9	Nafion 211	150	429	Nature Catalysis (2022)[40]
Fe_g–NC/Phen	3.5	Nafion 211	100	710	Energy & Environmental Science (2022)[49]
0.17 CVD/Fe–N–C-kat	4	Nafion 212	100	320	Angew. Chem., Int. Ed. (2020)[61]
Fe–AC–CVD	4	Nafion 212	100	601	Nature Energy (2022)[36]

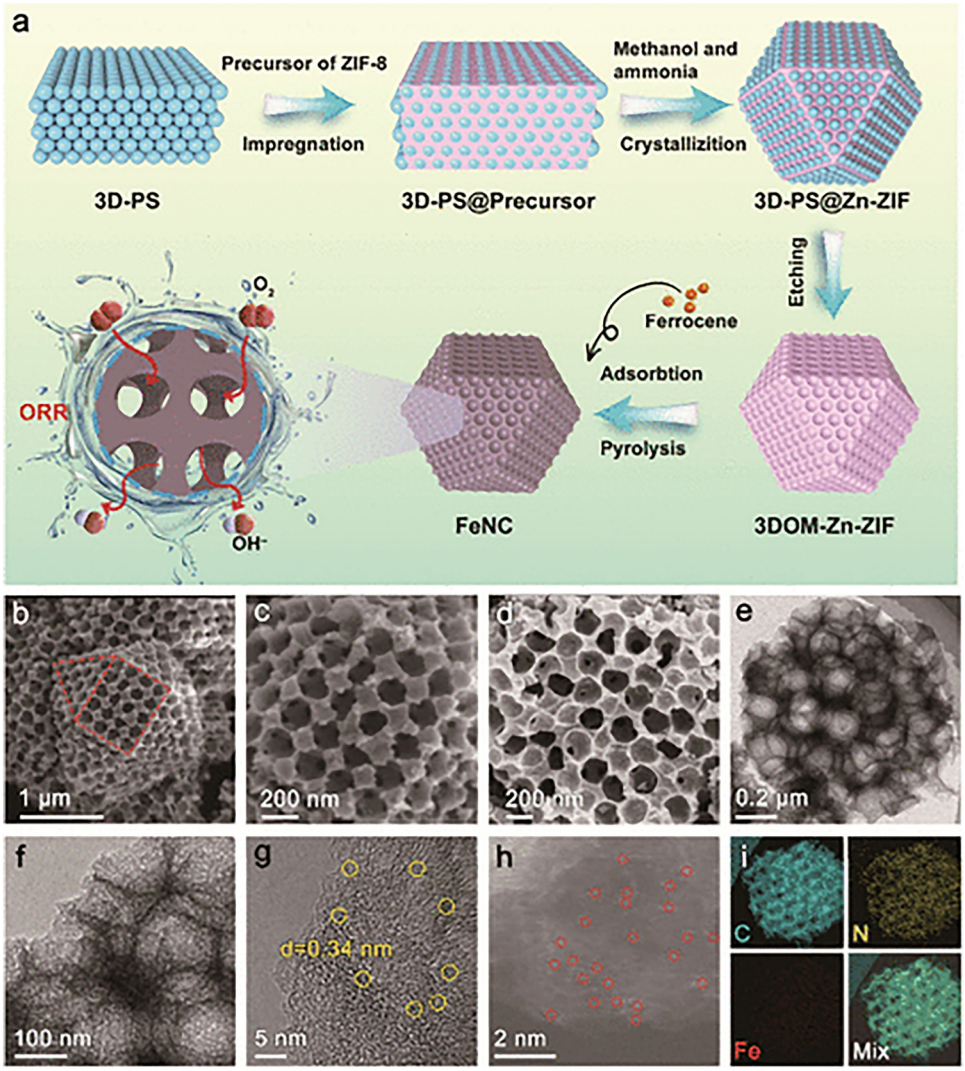

Fig. 6 Synthesis and structural characterization of FeNC catalysts. (a) Schematic illustration of the FeNC synthesis procedure. (b and c) SEM images of 3D-ordered macroporous Zn-doped ZIF precursor (3DOM-Zn-ZIF). (d) SEM image of the final FeNC-1000 catalyst. (e, f) TEM images, (g) high-resolution TEM (HRTEM), (h) aberration-corrected HAADF-STEM image showing isolated Fe atoms (highlighted with red circles), and (i) elemental mapping of FeNC-1000. Reproduce with permission.[67] Copyright © 2024 American Chemical Society.

rely on the self-assembly of surfactants or polymers to form pores during synthesis,[69] provide an simpler and cost effective synthesis route. One key advantage of soft templates is that they can typically be removed by simple solvent washing or low-temperature pyrolysis, while hard templates often require harsh chemical etching or high-temperature treatment. This makes soft templating more process-friendly and scalable. It is especially useful for improving the pore structure of ZIF-8-derived Fe–N–C materials, which usually have many micropores but very few mesopores. By introducing mesopores, soft-templating improves mass transport and increases the accessibility of Fe–N_x sites, which is important for thick catalyst layers. A variety of soft-templating agents—such as Pluronic F127, hexadecyl trimethyl ammonium bromide (CTAB), 1,3,5-trimethylbenzene (TMB), and 1H,1H,2H,2H-perfluorodecyltriethoxysilane (HFS)/oil—have been extensively studied,[59–61] and have been shown to significantly increase the mesopore ratio and surface area of the resulting catalysts (Fig. 7).[70–72]

4.2. Membrane electrode assemble optimization

Excluding the catalyst properties, the membrane electrode assembly (MEA) fabrication process also requires careful optimization, including parameters such as ionomer content and carbon additive amount. With respect to ionomer content, insufficient loading may result in poor coverage of the catalyst surface, limiting proton accessibility to the active sites and thereby reducing their effective utilization. Conversely, excessive ionomer can flood the porous structure, block oxygen transport channels and hindering reactant access to the active sites.[73,74] Pedersen *et al.* conducted a comprehensive study on ionomer loading optimization by correlating Fe–N–C pore size distribution with key electrochemical factors. Using advanced techniques including electrochemical impedance spectroscopy

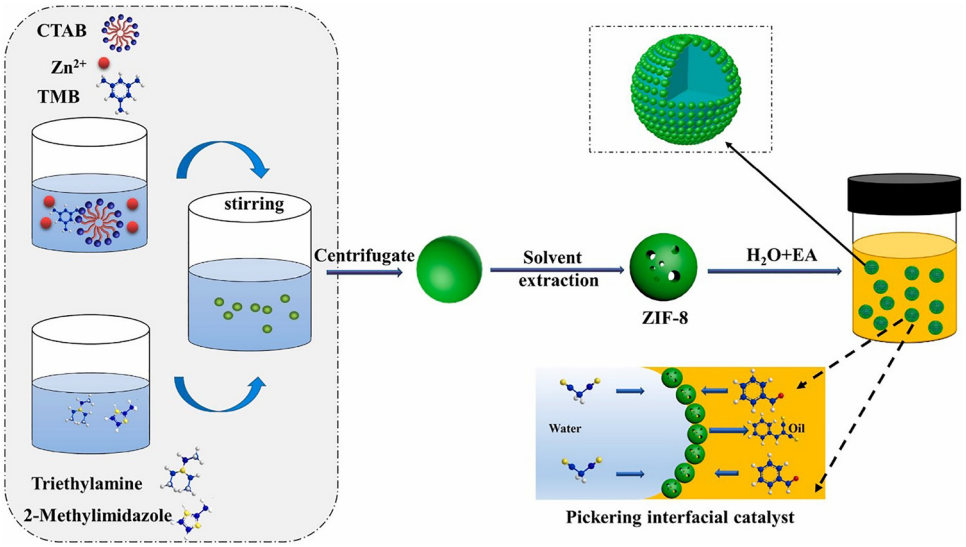

Fig. 7 Schematic of hierarchically porous ZIF-8 formation using TMB-induced pore expansion and Pickering emulsion templating. Reproduce with permission.[72] Copyright © 2021 Elsevier B.V.

(EIS), distribution of relaxation times (DRT), and Fourier-transformed alternating-current voltammetry (FTacV), they deconvoluted the contributions of proton resistance, electron resistance, and active site density to PEMFC performance, and proposed a novel quantitative evaluation framework.[75] This study provides valuable insights into the rational design and optimization of non-precious catalyst based MEAs, particularly emphasizing the critical role of the ionomer-to-carbon ratio in balancing proton conductivity and oxygen accessibility within the catalyst layer.

Carbon additives are particularly important in very thick non-precious metal catalyst layers. Although the treatments mentioned above can enhance the graphitization degree of Fe–N–C catalysts, their intrinsic conductivity remains substantially lower than that of conductive carbon blacks. This is primarily due to the presence of structural defects, amorphous carbon regions, and heteroatom doping (*e.g.*, nitrogen), which disrupt the extended π-conjugation network and hinder electron transport. As a result, insufficient conductivity in the catalyst layer can lead to pronounced voltage losses in the ohmic region.[76–78] In addition to enhancing conductivity, the use of different types of carbon black can further tailor the pore structure of the catalyst layer, thereby improving mass transport properties. Li *et al.* specifically investigated the impact of carbon fibre on PGM-free catalyst layer, showing that 7.5% of carbon fibre significantly reduced electronic resistance and improved PEMFC performance (60 mV at 1 A cm^{-2}) in high -resistivity catalyst layer.[79] In fact, carbon black is incorporated into the catalyst layer in most reported fuel cell studies involving Fe–N–C catalysts, as a means to improve electrical conductivity and support efficient catalyst utilization.[40,80]

Beyond catalyst and ink formulation, recent advances in gas diffusion layer (GDL) design have also shown promise in enhancing the performance of Fe–N–C-based MEAs. In particular, quadrilateral-patterned perforated GDLs have been reported to significantly improve oxygen transport and water management, both of which are critical for thick catalyst layers commonly required in non-precious metal systems.[81] Moreover, such hard templates mentioned above can be directly applied to the catalyst layer and later removed by solvent treatment to generate uniform macropores within the layer, which facilitates mass transport—especially in thick Fe–N–C catalyst layers. Although no direct studies have yet been reported for Fe–N–C systems, similar approaches have been extensively explored for catalyst layer engineering, mostly in the context of Pt/C-based electrodes.[82,83] These findings highlight the importance of structural engineering beyond active site design and suggest that integrating mass transport-enhancing strategies, originally developed for Pt-based systems, may hold great potential for further advancing Fe–N–C-based MEAs.

5. Limitations of RDE testing and the real-world relevance of Fe–N–C catalyst

In recent years, numerous Fe–N–C catalysts have demonstrated superior oxygen reduction activity in rotating disk electrode (RDE) tests, with some even exceeding the half-wave potentials of commercial Pt/C catalysts. However, when Fe–N–C catalysts are applied into PEMFCs, they often exhibit significantly poorer power densities and durability than their Pt-based catalysts. This contrast illustrates a fundamental disconnect between activity and fuel cell performance. The discrepancy arises from the vastly different reaction environments - RDE measurements reflect thin-film kinetics in a well-controlled electrolyte, while MEA operation involves complex mass transport, water management, ionomer interactions, and ohmic losses within a thick heterogeneous electrode. Understanding the cause of this performance gap is thus essential for translating laboratory

breakthroughs in Fe–N–C catalysis into realistic fuel cell application.

Recent studies highlight several strategies to bridge the performance gap between rotating disk electrode (RDE) tests and membrane electrode assembly (MEA) fuel cell performance for Fe–N–C catalysts. (1) Ionomer–catalyst interface optimization: improving the interaction between proton-conducting ionomer binders and Fe–N–C surfaces can greatly enhance catalyst utilization. For example, trace bromide doping of Fe–N–C was found to promote uniform ionomer coverage and penetration into catalyst particles, accelerating proton access and interfacial charge transfer.[38] (2) Hierarchical porous structure design: Engineering multi-scale porosity (micro-, meso-, and macropores) in Fe–N–C increases active site exposure while alleviating O_2 transport limitations. Introducing mesopores (*e.g. via* templating or chemical etching) yields smoother gas diffusion and has enabled record-high fuel cell power densities for single-atom Fe–N–C catalysts.[41,84,85] (3) Electrode thickness and compaction tuning: Optimising the catalyst layer thickness and its compaction (*e.g.* by calendaring) is critical for PGM-free cathodes. Fe–N–C cathodes typically require high loadings ($\sim$3–6 mg cm^{-2}) which, if too thick or poorly compacted, suffer from O_2 transport and proton diffusion resistances.[41] Careful control of layer thickness, porosity and compression can mitigate mass-transport losses while ensuring sufficient active site utilisation.

In addition to improving structure and interfaces of the catalyst layer, developing better electrochemical evaluation methods is crucial to accurately assess the practical performance of Fe–N–C catalysts in fuel cells. Two advanced half-cell techniques, the gas diffusion electrode (GDE) and the floating electrode (FE) method, have been developed to solve the limits of traditional RDE tests. Both the GDE and FE technique provide a more accurate assessment of catalyst performance than traditional RDE testing. Unlike RDE, which is limited by oxygen diffusion in liquid electrolyte, these techniques operate under high mass-transport conditions. GDE half-cell test effectively removes RDE diffusion limits by diffusing the gas through a Gas Diffusion Layer to the catalyst layer, providing reproducible and comparable activity data; this has now been extended to higher temperature and pressure conditions for more realistic PEMFC catalyst evaluation. The floating electrode technique is another half-cell technique which provides a more realistic way to test catalysts under high mass-transport conditions, much closer to how they actually work in fuel cells. The setup uses a thick polycarbonate track-etched (PCTE) membrane, about 12 μm thick, coated with a 100 nm gold layer to make it conductive. A very think catalyst film (around 0.6 μm) is deposited near the pores, which are made hydrophobic using PTFE. This structure creates a well-connected network which allows effective oxygen transfer and removal of water produced. The design also exhibits low electronic resistance and high proton conductivity.[85] Overall, the GDE test better reflects the real fuel cell operation by including ionomer effects and triple-phase boundaries, while the FE technique reveals the intrinsic catalytic activity of the material. Overall, they offer a more reliable evaluation of Fe–N–C catalyst behaviour, bridging the gap from half-cell to fuel cell (Fig. 8).

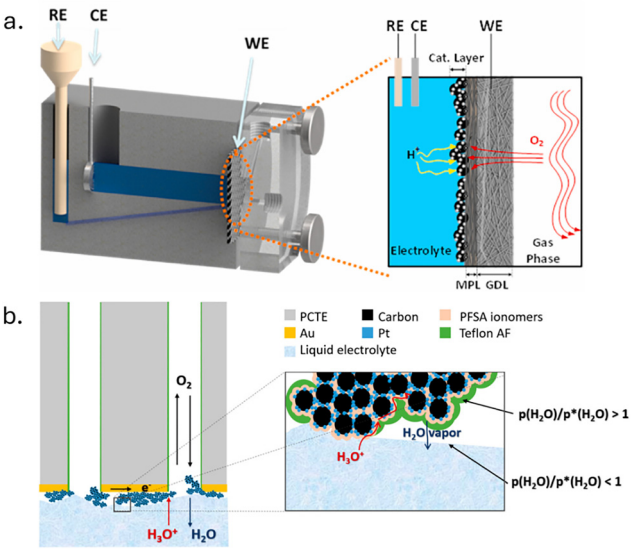

Fig. 8 Schematic configuration of (a) gas diffusion electrode (GDE) half-cell,[86] copyright © 2022 Elsevier B. V., (b) floating electrode (FE) half-cell,[85] copyright © 2020 American Chemical Society.

6. Summary and perspective

Although significant progress has been made in enhancing the activity and site density of Fe–N–C catalysts, their overall performance in proton exchange membrane fuel cells (PEMFCs) still falls short of practical requirements, particularly under high potentials and dynamic cycling conditions. As such, Fe–N–C remains far from commercial readiness. Nevertheless, due to their outstanding electrochemical properties, low cost, and structural tunability, Fe–N–C catalysts are still regarded as one of the most promising non-precious catalyst candidates for oxygen reduction reaction. To enable their widespread application in fuel cells, several critical issues must be addressed, including poor durability and limited mass transport property under real-world operating conditions.

Recent strategies, including hydrogen treatment, ammonia compounds, and nitrogen-rich additives, have achieved notable improvements in catalytic activity and stability. However, the scalability of large-scale production remains a major obstacle. Laboratory-scale synthesis methods, such as chemical vapor deposition (CVD), have proven effective in fabricating high-performance catalysts. Yet, translating these approaches into industrial-scale production—especially at the level of hundreds of grams of Fe–N–C materials, requires overcoming barriers related to precursor cost, reactor size and design limitations, waste disposal and ensuring consistent catalyst quality. In contrast, the impregnation–pyrolysis route is, at present, the most practical pathway for scaling high-loading, high-performance Fe–N–C catalysts—particularly when coupled with the Section 2 strategies (*e.g.*, coordination/environment tuning)

and the Section 4 hierarchical porosity engineering, offering a comparatively straightforward path to larger-scale production.

Looking forward, research efforts should move beyond material-level activity optimization toward the rational design of hierarchical porous structures and integrated optimization of membrane electrode assemblies (MEAs). Constructing micro-, meso-, and macro-porous networks within Fe–N–C catalysts can synergistically promote reactant adsorption, ion diffusion, and gas transport across multiple length scales, thereby alleviating mass transfer limitations and significantly enhancing catalytic efficiency and durability under realistic fuel cell operation. Moreover, precise engineering of the triple phase interface, coupled with the application of advanced *in situ* characterization techniques to reveal degradation pathways practically, will be critical for ensuring long-term operational stability. In addition, addressing scalability and catalyst evaluation method developed are crucial. Process optimization, the use of low-cost precursors, and the establishment of standardized testing protocols will play import roles in narrowing the gap between laboratory research and commercial application.

Finally, the successful deployment of Fe–N–C catalysts in fuel cells will depend not only on the design of active sites but also on the engineering of hierarchical porous architectures, integrated with multidisciplinary engineering solutions to guarantee durability and economic viability. As these challenges are progressively resolved, Fe–N–C catalysts hold great promise in advancing next-generation clean energy technologies and accelerating the global transition toward carbon neutrality.

Conflicts of interest

The authors declare that they have no known competing financial interests or personal relationships that could have appeared to influence the work reported in this paper.

Data availability

This article is a perspective/review and does not include new experimental data. All data supporting the discussion are available in the cited literature. No additional datasets were generated or analyzed for this work. All figures or data directly reproduced from previous publications have been used with proper permission from the copyright holders.

Acknowledgements

The authors would like to acknowledge the financial support from the EPSRC (EP/W033321/1, EP/S018204/2, EP/P009050/1 and EP/R023581/1) for supporting the Electrochemical Innovation Lab.

References

1 A. Zecca and L. Chiari, Fossil-fuel constraints on global warming, *Energy Policy*, 2010, **38**(1), 1–3.
2 IEA. *Power systems in transition: Challenges and opportunities ahead for electricity security*, Paris, 2020.
3 T. Yoshida and K. Kojima, Toyota MIRAI Fuel Cell Vehicle and Progress Toward a Future Hydrogen Society, *Electrochem. Soc. Interface.*, 2015, **24**(2), 45.
4 G. K. Adria Wilson and D. Papageorgopoulos. *DOE Hydrogen and Fuel Cells Program Record*. 2017.
5 R. Jasinski, A New Fuel Cell Cathode Catalyst, *Nature*, 1964, **201**(4925), 1212–1213.
6 R. Jasinski, Cobalt Phthalocyanine as a Fuel Cell Cathode, *J. Electrochem. Soc.*, 1965, **112**(5), 526.
7 R. Cheng, X. He, M. Jiang, X. Shao, W. Tang, B. Ran, H. Li and C. Fu, f-p-d Gradient Orbital Coupling Induced Spin State Enhancement of Atomic Fe Sites for Efficient and Stable Oxygen Reduction Reaction, *Adv. Funct. Mater.*, 2025, 2425138.
8 S. Yang, A. Verdaguer-Casadevall, L. Arnarson, L. Silvioli, V. Čolić, R. Frydendal, J. Rossmeisl, I. Chorkendorff and I. E. L. Stephens, Toward the Decentralized Electrochemical Production of H2O2: A Focus on the Catalysis, *ACS Catal.*, 2018, **8**(5), 4064–4081.
9 A. Pedersen, J. Barrio, A. Li, R. Jervis, D. J. L. Brett, M. M. Titirici and I. E. L. Stephens, Dual-Metal Atom Electrocatalysts: Theory, Synthesis, Characterization, and Applications, *Adv. Energy Mater.*, 2022, **12**(3), 2102715.
10 Y. Shao, J.-P. Dodelet, G. Wu and P. Zelenay, PGM-Free Cathode Catalysts for PEM Fuel Cells: A Mini-Review on Stability Challenges, *Adv. Mater.*, 2019, **31**(31), 1807615.
11 L. Du, V. Prabhakaran, X. Xie, S. Park, Y. Wang and Y. Shao, Low-PGM and PGM-Free Catalysts for Proton Exchange Membrane Fuel Cells: Stability Challenges and Material Solutions, *Adv. Mater.*, 2021, **33**(6), 1908232.
12 H. Li, Y. Wen, M. Jiang, Y. Yao, H. Zhou, Z. Huang, J. Li, S. Jiao, Y. Kuang and S. Luo, Understanding of Neighboring Fe-N4-C and Co-N4-C Dual Active Centers for Oxygen Reduction Reaction, *Adv. Funct. Mater.*, 2021, **31**(22), 2011289.
13 J. Qiao, C. Lu, L. Kong, J. Zhang, Q. Lin, H. Huang, C. Li, W. He, M. Zhou and Z. Sun, Spin Engineering of Fe–N–C by Axial Ligand Modulation for Enhanced Bifunctional Oxygen Catalysis, *Adv. Funct. Mater.*, 2024, **34**(51), 2409794.
14 J. Weiss, H. Zhang and P. Zelenay, Recent progress in the durability of Fe-N-C oxygen reduction electrocatalysts for polymer electrolyte fuel cells, *J. Electroanal. Chem.*, 2020, **875**, 114696.
15 J. Bai, T. Zhao, M. Xu, B. Mei, L. Yang, Z. Shi, S. Zhu, Y. Wang, Z. Jiang, J. Zhao, J. Ge, M. Xiao, C. Liu and W. Xing, Monosymmetric Fe-N4 sites enabling durable proton exchange membrane fuel cell cathode by chemical vapor modification, *Nat. Commun.*, 2024, **15**(1), 4219.
16 K. Kumar, L. Dubau, F. Jaouen and F. Maillard, Review on the Degradation Mechanisms of Metal-N-C Catalysts for the Oxygen Reduction Reaction in Acid Electrolyte: Current Understanding and Mitigation Approaches, *Chem. Rev.*, 2023, **123**(15), 9265–9326.
17 D. Banham, T. Kishimoto, Y. Zhou, T. Sato, K. Bai, J-i Ozaki, Y. Imashiro and S. Ye, Critical advancements in achieving high power and stable nonprecious metal catalyst–based

MEAs for real-world proton exchange membrane fuel cell applications, *Sci. Adv.*, 2018, **4**(3), eaar7180.

18 V. P. Glibin, M. Cherif, F. Vidal, J.-P. Dodelet, G. Zhang and S. Sun, Non-PGM Electrocatalysts for PEM Fuel Cells: Thermodynamic Stability and DFT Evaluation of Fluorinated FeN4-Based ORR Catalysts, *J. Electrochem. Soc.*, 2019, **166**(7), F3277.

19 S. Pérez-Rodríguez, D. Sebastián and M. J. Lázaro, Electrochemical oxidation of ordered mesoporous carbons and the influence of graphitization, *Electrochim. Acta*, 2019, **303**, 167–175.

20 S. Wang, A Comparative study of Fenton and Fenton-like reaction kinetics in decolourisation of wastewater, *Dyes Pigm.*, 2008, **76**(3), 714–720.

21 X. Yin and P. Zelenay, (Invited) Kinetic Models for the Degradation Mechanisms of PGM-Free ORR Catalysts, *ECS Trans.*, 2018, **85**(13), 1239.

22 Y. Zeng, C. Li, B. Li, J. Liang, M. J. Zachman, D. A. Cullen, R. P. Hermann, E. E. Alp, B. Lavina, S. Karakalos, M. Lucero, B. Zhang, M. Wang, Z. Feng, G. Wang, J. Xie, D. J. Myers, J.-P. Dodelet and G. Wu, Tuning the thermal activation atmosphere breaks the activity–stability trade-off of Fe–N–C oxygen reduction fuel cell catalysts, *Nat. Catal.*, 2023, **6**(12), 1215–1227.

23 J. P. Masnica, S. Sibt-e-Hassan, S. Potgieter-Vermaak, Y. N. Regmi, L. A. King and L. Tosheva, ZIF-8-derived Fe-C catalysts: Relationship between structure and catalytic activity toward the oxygen reduction reaction, *Green Carbon*, 2023, **1**(2), 160–169.

24 E. Proietti, F. Jaouen, M. Lefèvre, N. Larouche, J. Tian, J. Herranz and J.-P. Dodelet, Iron-based cathode catalyst with enhanced power density in polymer electrolyte membrane fuel cells, *Nat. Commun.*, 2011, **2**(1), 416.

25 L. Gao, M. Xiao, Z. Jin, C. Liu, J. Ge and W. Xing, Hydrogen etching induced hierarchical meso/micro-pore structure with increased active density to boost ORR performance of Fe-N-C catalyst, *J. Energy Chem.*, 2019, **35**, 17–23.

26 F. Jaouen, M. Lefèvre, J.-P. Dodelet and M. Cai, Heat-Treated Fe/N/C Catalysts for O2 Electroreduction: Are Active Sites Hosted in Micropores?, *J. Phys. Chem. B*, 2006, **110**(11), 5553–5558.

27 S. R. Arsad, P. J. Ker, M. A. Hannan, S. G. H. Tang, R. S. N. Chau and C. F. Mahlia, TMI. Patent landscape review of hydrogen production methods: Assessing technological updates and innovations, *Int. J. Hydrogen Energy*, 2024, **50**, 447–472.

28 H. Tabassum, S. Mukherjee, J. Chen, D. Holiharimanana, S. Karakalos, X. Yang, S. Hwang, T. Zhang, B. Lu, M. Chen, Z. Tang, E. A. Kyriakidou, Q. Ge and G. Wu, Hydrogen generation via ammonia decomposition on highly efficient and stable Ru-free catalysts: approaching complete conversion at 450 °C, *Energy Environ. Sci.*, 2022, **15**(10), 4190–4200.

29 M. Lefèvre, E. Proietti, F. Jaouen and J.-P. Dodelet, Iron-Based Catalysts with Improved Oxygen Reduction Activity in Polymer Electrolyte Fuel Cells, *Science*, 2009, **324**(5923), 71–74.

30 U. I. Kramm, I. Herrmann-Geppert, P. Bogdanoff and S. Fiechter, Effect of an Ammonia Treatment on Structure, Composition, and Oxygen Reduction Reaction Activity of Fe–N–C Catalysts, *J. Phys. Chem. C*, 2011, **115**(47), 23417–23427.

31 C. Yan, Y. Ye, L. Lin, H. Wu, Q. Jiang, G. Wang and X. Bao, Improving CO2 electroreduction over ZIF-derived carbon doped with Fe-N sites by an additional ammonia treatment, *Catal. Today*, 2019, **330**, 252–258.

32 L. Costa and G. Camino, Thermal behaviour of melamine, *J. Therm. Anal.*, 1988, **34**(2), 423–429.

33 Y. Li, S. Yin, L. Chen, X. Cheng, C. Wang, Y. Jiang and S. Sun, Boost the Utilization of Dense FeN4 Sites for High-Performance Proton Exchange Membrane Fuel Cells, *Energy Environ. Mater.*, 2024, **7**(3), e12611.

34 Y. Li, S. Yin, L. Chen, X. Cheng, C. Wang, Y. Jiang and S. Sun, Boost the Utilization of Dense FeN Sites for High-Performance Proton Exchange Membrane Fuel Cells, *Energy Environ. Mater.*, 2024, **7**(3), e12611.

35 T. Marshall-Roth, N. J. Libretto, A. T. Wrobel, K. J. Anderton, M. L. Pegis, N. D. Ricke, T. V. Voorhis, J. T. Miller and Y. Surendranath, A pyridinic Fe-N4 macrocycle models the active sites in Fe/N-doped carbon electrocatalysts, *Nat. Commun.*, 2020, **11**(1), 5283.

36 S. Liu, C. Li, M. J. Zachman, Y. Zeng, H. Yu, B. Li, M. Wang, J. Braaten, J. Liu, H. M. Meyer, M. Lucero, A. J. Kropf, E. E. Alp, Q. Gong, Q. Shi, Z. Feng, H. Xu, G. Wang, D. J. Myers, J. Xie, D. A. Cullen, S. Litster and G. Wu, Atomically dispersed iron sites with a nitrogen–carbon coating as highly active and durable oxygen reduction catalysts for fuel cells, *Nat. Energy*, 2022, **7**(7), 652–663.

37 J. Liu, Y. Liu, B. Nan, D. Wang, C. Allen, Z. Gong, G. He, K. Fu, G. Ye and H. Fei, A Two-in-One Strategy to Simultaneously Boost the Site Density and Turnover Frequency of Fe−N−C Oxygen Reduction Catalysts, *Angew. Chem., Int. Ed.*, 2025, **64**(14), e202425196.

38 S. Yin, L. Chen, J. Yang, X. Cheng, H. Zeng, Y. Hong, H. Huang, X. Kuai, Y. Lin, R. Huang, Y. Jiang and S. Sun, A Fe-NC electrocatalyst boosted by trace bromide ions with high performance in proton exchange membrane fuel cells, *Nat. Commun.*, 2024, **15**(1), 7489.

39 X. Yan, Y. Yao and Y. Chen, Highly Active and Stable Fe-N-C Oxygen Reduction Electrocatalysts Derived from Electrospinning and In Situ Pyrolysis, *Nanoscale Res. Lett.*, 2018, **13**(1), 218.

40 A. Mehmood, M. Gong, F. Jaouen, A. Roy, A. Zitolo, A. Khan, M.-T. Sougrati, M. Primbs, A. M. Bonastre, D. Fongalland, G. Drazic, P. Strasser and A. Kucernak, High loading of single atomic iron sites in Fe–NC oxygen reduction catalysts for proton exchange membrane fuel cells, *Nat. Catal.*, 2022, **5**(4), 311–323.

41 Q. Ma, H. Jin, J. Zhu, Z. Li, H. Xu, B. Liu, Z. Zhang, J. Ma and S. Mu, Stabilizing Fe-N-C Catalysts as Model for Oxygen Reduction Reaction, *Adv. Sci.*, 2021, **8**(23), e2102209.

42 J. Y. Cheon, J. H. Kim, J. H. Kim, K. C. Goddeti, J. Y. Park and S. H. Joo, Intrinsic Relationship between Enhanced Oxygen Reduction Reaction Activity and Nanoscale Work

Function of Doped Carbons, *J. Am. Chem. Soc.*, 2014, **136**(25), 8875–8878.

43 U. Tylus, Q. Jia, K. Strickland, N. Ramaswamy, A. Serov, P. Atanassov and S. Mukerjee, Elucidating Oxygen Reduction Active Sites in Pyrolyzed Metal–Nitrogen Coordinated Non-Precious-Metal Electrocatalyst Systems, *J. Phys. Chem. C*, 2014, **118**(17), 8999–9008.

44 M. Ferrandon, A. J. Kropf, D. J. Myers, K. Artyushkova, U. Kramm, P. Bogdanoff, G. Wu, C. M. Johnston and P. Zelenay, Multitechnique Characterization of a Polyaniline–Iron–Carbon Oxygen Reduction Catalyst, *J. Phys. Chem. C*, 2012, **116**(30), 16001–16013.

45 Y. Gao, Z. Cai, X. Wu, Z. Lv, P. Wu and C. Cai, Graphdiyne-Supported Single-Atom-Sized Fe Catalysts for the Oxygen Reduction Reaction: DFT Predictions and Experimental Validations, *ACS Catal.*, 2018, **8**(11), 10364–10374.

46 S. Lv, H. Wang, Y. Zhou, D. Tang and S. Bi, Recent advances in heterogeneous single-atom nanomaterials: From engineered metal-support interaction to applications in sensors, *Coord. Chem. Rev.*, 2023, **478**, 214976.

47 X.-F. Yang, A. Wang, B. Qiao, J. Li, J. Liu and T. Zhang, Single-Atom Catalysts: A New Frontier in Heterogeneous Catalysis, *Acc. Chem. Res.*, 2013, **46**(8), 1740–1748.

48 L. Sun, G. Yuan, L. Gao, J. Yang, M. Chhowalla, M. H. Gharahcheshmeh, K. K. Gleason, Y. S. Choi, B. H. Hong and Z. Liu, Chemical vapour deposition, *Nat. Rev. Methods Primers*, 2021, **1**(1), 5.

49 S.-H. Yin, S.-L. Yang, G. Li, G. Li, B.-W. Zhang, C.-T. Wang, M.-S. Chen, H.-G. Liao, J. Yang, Y.-X. Jiang and S.-G. Sun, Seizing gaseous Fe2+ to densify O2-accessible Fe–N4 sites for high-performance proton exchange membrane fuel cells, *Energy Environ. Sci.*, 2022, **15**(7), 3033–3040.

50 L. Jiao, J. Li, L. L. Richard, Q. Sun, T. Stracensky, E. Liu, M. T. Sougrati, Z. Zhao, F. Yang, S. Zhong, H. Xu, S. Mukerjee, Y. Huang, D. A. Cullen, J. H. Park, M. Ferrandon, D. J. Myers, F. Jaouen and Q. Jia, Chemical vapour deposition of Fe–N–C oxygen reduction catalysts with full utilization of dense Fe–N4 sites, *Nat. Mater.*, 2021, **20**(10), 1385–1391.

51 X. Yang, B. Zhu, Z. Gao, C. Yang, J. Zhou, A. Han and J. Liu, A Vacuum Vapor Deposition Strategy to Fe Single-Atom Catalysts with Densely Active Sites for High-Performance Zn–Air Battery, *Adv. Sci.*, 2024, **11**(34), 2306594.

52 L. Gao, M. Xiao, Z. Jin, C. Liu, J. Zhu, J. Ge and W. Xing, Correlating Fe source with Fe-N-C active site construction: Guidance for rational design of high-performance ORR catalyst, *J. Energy Chem.*, 2018, **27**(6), 1668–1673.

53 S. Ji, Y. Chen, X. Wang, Z. Zhang, D. Wang and Y. Li, Chemical Synthesis of Single Atomic Site Catalysts, *Chem. Rev.*, 2020, **120**(21), 11900–11955.

54 D. Cai, J. Zhang, Z. Kong and Z. Li, Synergistic Effect of Single-Atom Catalysts and Vacancies of Support for Versatile Catalytic Applications, *ChemCatChem*, 2024, **16**(18), e202301414.

55 Z. Xu, G. Chen, F. Yang, J. Jang, G. Liu, F. Xiao, Y. Sun, X. Qiu, W. Chen, D. Su, M. Gu and M. Shao, Graphene-supported Fe/Ni single atoms and FeNi alloy nanoparticles as bifunctional oxygen electrocatalysts for rechargeable zinc-air batteries, *Electrochim. Acta*, 2023, **458**, 142549.

56 X. Lu, Y. Li, P. Yang, Y. Wan, D. Wang, H. Xu, L. Liu, L. Xiao, R. Li, G. Wang, J. Zhang, M. An and G. Wu, Atomically dispersed Fe-N-C catalyst with densely exposed Fe-N4 active sites for enhanced oxygen reduction reaction, *Chem. Eng. J.*, 2024, **485**, 149529.

57 L. Lan, Y. Wu, Y. Pei, Y. Wei, T. Hu, D. Lützenkirchen-Hecht, K. Yuan and Y. Chen, High-Density Accessible Iron Single-Atom Catalyst for Durable and Temperature-Adaptive Laminated Zinc-Air Batteries, *Adv. Mater.*, 2025, **37**(11), 2417711.

58 X. Hai, S. Xi, S. Mitchell, K. Harrath, H. Xu, D. F. Akl, D. Kong, J. Li, Z. Li, T. Sun, H. Yang, Y. Cui, C. Su, X. Zhao, J. Li, J. Pérez-Ramírez and J. Lu, Scalable two-step annealing method for preparing ultra-high-density single-atom catalyst libraries, *Nat. Nanotechnol.*, 2022, **17**(2), 174–181.

59 Á. García, T. Haynes, M. Retuerto, P. Ferrer, L. Pascual, M. A. Peña, M. Abdel Salam, M. Mokhtar, D. Gianolio and S. Rojas, Effect of the Thermal Treatment of Fe/N/C Catalysts for the Oxygen Reduction Reaction Synthesized by Pyrolysis of Covalent Organic Frameworks, *Ind. Eng. Chem. Res.*, 2021, **60**(51), 18759–18769.

60 U. I. Kramm, A. Zana, T. Vosch, S. Fiechter, M. Arenz and D. Schmeißer, On the structural composition and stability of Fe–N–C catalysts prepared by an intermediate acid leaching, *J. Solid State Electrochem.*, 2016, **20**(4), 969–981.

61 S. Liu, M. Wang, X. Yang, Q. Shi, Z. Qiao, M. Lucero, Q. Ma, K. L. More, D. A. Cullen, Z. Feng and G. Wu, Chemical Vapor Deposition for Atomically Dispersed and Nitrogen Coordinated Single Metal Site Catalysts, *Angew. Chem., Int. Ed.*, 2020, **59**(48), 21698–21705.

62 D. Kim, J. Park, S. Jung, J. Jang, M. Han, M. Kim, W. Zhu, W.-J. Song, Y. Yamauchi and J. Kim, Study on the importance of uniformity and nanoparticle size in ZIF-8 carbon nanoarchitecture for enhancing electrochemical properties, *Nanoscale*, 2025, **17**(16), 10344–10355.

63 H. Huang, J.-R. Li, K. Wang, T. Han, M. Tong, L. Li, Y. Xie, Q. Yang, D. Liu and C. Zhong, An in situ self-assembly template strategy for the preparation of hierarchical-pore metal-organic frameworks, *Nat. Commun.*, 2015, **6**(1), 8847.

64 M. Marcos-Hernández and D. Villagrán, in 11 - Mesoporous Composite Nanomaterials for Dye Removal and Other Applications, ed G. Z. Kyzas, A. C. Mitropoulos, *Composite Nanoadsorbents*, Elsevier, 2019, p. 265–293.

65 K. Shen, L. Zhang, X. Chen, L. Liu, D. Zhang, Y. Han, J. Chen, J. Long, R. Luque, Y. Li and B. Chen, Ordered macro-microporous metal-organic framework single crystals, *Science*, 2018, **359**(6372), 206–210.

66 C. Zhao, G.-L. Xu, Z. Yu, L. Zhang, I. Hwang, Y.-X. Mo, Y. Ren, L. Cheng, C.-J. Sun, Y. Ren, X. Zuo, J.-T. Li, S.-G. Sun, K. Amine and T. Zhao, Author Correction: A high-energy and long-cycling lithium–sulfur pouch cell via a macroporous catalytic cathode with double-end binding sites, *Nat. Nanotechnol.*, 2021, **16**(2), 224.

67 W. Zhai, J. Li, Y. Tian, H. Liu, Y. Liu, Z. Guo, T. Sakthivel, L. Bai, X.-F. Yu and Z. Dai, Consolidating the Oxygen

Reduction with Sub-Polarized Graphitic Fe–N4 Atomic Sites for an Efficient Flexible Zinc–Air Battery, *Nano Lett.*, 2024, **24**(46), 14632–14640.

68 M. Xie, Y. Lu, X. Xiao, D. Wu, B. Shao, H. Nian, C. Wu, W. Wang, J. Gu, S. Han, M. Gu and Q. Xu, Spatially Immobilized PtPdFeCoNi as an Excellent Bifunctional Oxygen Electrocatalyst for Zinc–Air Battery, *Adv. Funct. Mater.*, 2024, 2414537.

69 B. Ghritalahre, V. K. Bhargav, S. Gangil, P. Sahu and R. K. Sahu, Next generation bio-derived 3D-hierarchical porous material for remarkable hydrogen storage – A brief critical review, *J. Power Sources*, 2023, **587**, 233648.

70 F. S. Butt, A. Lewis, R. Rea, N. A. Mazlan, T. Chen, N. Radacsi, E. Mangano, X. Fan, Y. Yang, S. Yang and Y. Huang, Highly-Controlled Soft-Templating Synthesis of Hollow ZIF-8 Nanospheres for Selective CO2 Separation and Storage, *ACS Appl. Mater. Interfaces*, 2023, **15**(26), 31740–31754.

71 Y. Mun, M. J. Kim, S.-A. Park, E. Lee, Y. Ye, S. Lee, Y.-T. Kim, S. Kim, O.-H. Kim, Y.-H. Cho, Y.-E. Sung and J. Lee, Soft-template synthesis of mesoporous non-precious metal catalyst with Fe-Nx/C active sites for oxygen reduction reaction in fuel cells, *Appl. Catal., B*, 2018, **222**, 191–199.

72 Z. Guo, W. Li, W. Li, X. Hou, S. Luan, Y. Song and Q. Wang, Hierarchically porous zeolitic imidazolate framework-8 with tunable mesostructure as Pickering interfacial catalyst, *Microporous Mesoporous Mater.*, 2021, **310**, 110677.

73 H. Ren, Y. Teng, X. Meng, D. Fang, H. Huang, J. Geng and Z. Shao, Ionomer network of catalyst layers for proton exchange membrane fuel cell, *J. Power Sources*, 2021, **506**, 230186.

74 A. Pedersen, R. Z. Snitkoff-Sol, Y. Presman, L. Dubau, R. Cai, J. Barrio, S. J. Haigh, F. Maillard, I. E. L. Stephens, M.-M. Titirici and L. Elbaz, Fe-N-C in Proton Exchange Membrane Fuel Cells: Impact of Ionomer Loading on Degradation and Stability, *Adv. Energy Mater.*, 2024, 2403920.

75 A. Pedersen, R. Z. Snitkoff-Sol, Y. Presman, J. Barrio, R. Cai, T. Suter, G. Yang, S. J. Haigh, D. Brett, R. Jervis, M.-M. Titirici, I. E. L. Stephens and L. Elbaz, Optimisation and effect of ionomer loading on porous Fe–N–C-based proton exchange membrane fuel cells probed by emerging electrochemical methods, *J. Power Sources*, 2024, **609**, 234683.

76 F. Jaouen, E. Proietti, M. Lefèvre, R. Chenitz, J.-P. Dodelet, G. Wu, H. T. Chung, C. M. Johnston and P. Zelenay, Recent advances in non-precious metal catalysis for oxygen-reduction reaction in polymer electrolyte fuel cells, *Energy Environ. Sci.*, 2011, **4**(1), 114–130.

77 T. Reshetenko, A. Serov, M. Odgaard, G. Randolf, L. Osmieri and A. Kulikovsky, Electron and proton conductivity of Fe-N-C cathodes for PEM fuel cells: A model-based electrochemical impedance spectroscopy measurement, *Electrochem. Commun.*, 2020, **118**, 106795.

78 J.-S. Choi, W. S. Chung, H. Y. Ha, T.-H. Lim, I.-H. Oh, S.-A. Hong and H.-I. Lee, Nano-structured Pt–Cr anode catalyst over carbon support, for direct methanol fuel cell, *J. Power Sources*, 2006, **156**(2), 466–471.

79 Y.-S. Li, D. Menga, H. A. Gasteiger and B. Suthar, Design of PGM-Free Cathode Catalyst Layers for PEMFC Applications: The Impact of Electronic Conductivity, *J. Electrochem. Soc.*, 2023, **170**(9), 094503.

80 H. Adabi, A. Shakouri, N. Ul Hassan, J. R. Varcoe, B. Zulevi, A. Serov, J. R. Regalbuto and W. E. Mustain, High-performing commercial Fe–N–C cathode electrocatalyst for anion-exchange membrane fuel cells, *Nat. Energy*, 2021, **6**(8), 834–843.

81 P. Lin, J. Sun, C. He, M. Wu and T. Zhao, Quadrilateral-Patterned Perforated Gas Diffusion Layers Boost the Performance of Fuel Cells, *ACS Energy Lett.*, 2024, **9**(4), 1710–1716.

82 A. Zlotorowicz, K. Jayasayee, P. I. Dahl, M. S. Thomassen and S. Kjelstrup, Tailored porosities of the cathode layer for improved polymer electrolyte fuel cell performance, *J. Power Sources*, 2015, **287**, 472–477.

83 Y.-H. Cho, N. Jung, Y. S. Kang, D. Y. Chung, J. W. Lim, H. Choe, Y.-H. Cho and Y.-E. Sung, Improved mass transfer using a pore former in cathode catalyst layer in the direct methanol fuel cell, *Int. J. Hydrogen Energy*, 2012, **37**(16), 11969–11974.

84 Y. Zhao, J. Wan, C. Ling, Y. Wang, H. He, N. Yang, R. Wen, Q. Zhang, L. Gu, B. Yang, Z. Xiang, C. Chen, J. Wang, X. Wang, Y. Wang, H. Tao, X. Li, B. Liu, S. Zhang and D. Wang, Acidic oxygen reduction by single-atom Fe catalysts on curved supports, *Nature*, 2025, **644**(8077), 668–675.

85 X. Lin, C. M. Zalitis, J. Sharman and A. Kucernak, Electrocatalyst Performance at the Gas/Electrolyte Interface under High-Mass-Transport Conditions: Optimization of the ''Floating Electrode'' M5ethod, *ACS Appl. Mater. Interfaces*, 2020, **12**(42), 47467–47481.

86 N. Schmitt, M. Schmidt, G. Hübner and B. J. M. Etzold, Oxygen reduction reaction measurements on platinum electrocatalysts in gas diffusion electrode half-cells: Influence of electrode preparation, measurement protocols and common pitfalls, *J. Power Sources*, 2022, **539**, 231530.